Journal of Applied Polymer Science

Thermal property, morphology, and hydrolysis ability of poly(lactic acid)/chitosan nanocomposites using polyethylene oxide

Nguyen Thuy Chinh,[1] Nguyen Thi Thu Trang,[1] Dinh Thi Mai Thanh,[1] To Thi Xuan Hang,[1] Nguyen Vu Giang,[1] Pham Minh Quan,[2] Nguyen Tien Dung,[3] Thai Hoang[1]

[1]Institute for Tropical Technology, Vietnam Academy of Science and Technology, 18 Hoang Quoc Viet, Cau Giay, Ha Noi, Vietnam
[2]Institute of Natural Products Chemistry, Vietnam Academy of Science and Technology, 18 Hoang Quoc Viet, Cau Giay, Hanoi, Vietnam
[3]Faculty of Chemistry, Hanoi National University of Education, 136 Xuan Thuy, Cau Giay, Hanoi, Vietnam
Correspondence to: T. Hoang (E-mail: hoangth@itt.vast.vn)

ABSTRACT: Poly(lactic acid) (PLA) and chitosan (CS) are two natural resource polymers, which have been applied widely into different fields. Polymer composites based on PLA and CS have some advantages such as good adhesion, biodegradability, biocompatibility, and high stability. They can be prepared by different methods including the solution, emulsion, and electrospinning methods. In this work, the PLA/chitosan nanocomposites were prepared by solution method using poly(ethylene oxide) (PEO) as a compatibilizer in order to improve interaction and dispersion between PLA and CS phases. The characterization and morphology of the above nanocomposites were determined by Fourier Transform Infrared Spectroscopy (FTIR), thermograviety analysis, differential scanning calorimetry, and scanning electron microscopy. Hydrolysis ability of PLA/CS nanocomposites with and without PEO was also investigated in acid and phosphate buffer solutions. The obtained results showed the compatibility between PLA and CS phases in the PLA/CS nanocomposites using PEO was improved clearly and weight loss of PLA/CS/PEO nanocomposites in the above environments lower than that of PLA/CS nanocomposites. © 2014 Wiley Periodicals, Inc. J. Appl. Polym. Sci. **2015**, *132*, 41690.

KEYWORDS: biodegradable; biopolymers and renewable polymers; blends; composites; thermal properties

Received 5 August 2014; accepted 29 October 2014
DOI: 10.1002/app.41690

INTRODUCTION

Chitosan (CS) has one primary amino and two free hydroxyl groups for each C6 building unit. Because of excellent biological properties of CS such as biodegradability, nontoxicity, antibacterial ability, and biocompatibility, CS and composite materials based on CS have been known as promising material in many biomedical fields from skin to bone or cartilage.[1] However, CS has poor mechanical strength and insoluble in water and organic solvents, especially, CS hydrolysis might happen under the conditions of water or tissue fluid.[2]

The hydrophobic polyester as poly(lactic acid) (PLA) has good mechanical property, biodegradability, biocompatibility, and the ability to be dissolved in common solvents. Besides, PLA also has disadvantages such as brittle, easy to break, poor elongation, high cost.[3] Therefore, the application of PLA in some fields can be limited.

Blending CS with PLA is expected to form new biomaterial exhibiting combinations of properties that could not be obtained by individual polymers. This composite is promised to achieve a better biodegradable, biocompatible, mechanical strength, and elongation, etc. In several previous reports, the morphology and dispersibility of PLA/CS composites were presented and discussed.[4–9] The obtained results showed that the difference in nature, structure, and compatibility between PLA and CS can lead to the poor dispersion of two phases. Therefore, using compatibilizers such as poly(ethylene oxide) (PEO), poly(caprolactone) (PCL), poly(ethylene glycol) (PEG) was carried out to improve dispersibility and compatibility between CS and PLA.[10–13] Rajan *et al.* used PEG as a emulsifier with a big amount for PLA-CS-gelatin composites to apply for Rifampicin delivery.[11] The FTIR, surface morphology of CS-PLA-PEO-gelatin nanoparticles including the particle size were studied. The obtained results showed these nanoparticles as new potential systems for controlled drug delivery. In our previous work,[13] the morphology, compatibility, and hydrolysis of PLA/CS composites with PEG compatibilizer have been studied. The results also indicated PEG can significantly enhance the dispersion between PLA and CS thanks to the OH and C—O—C groups in PEG molecules having the ability to interact with the

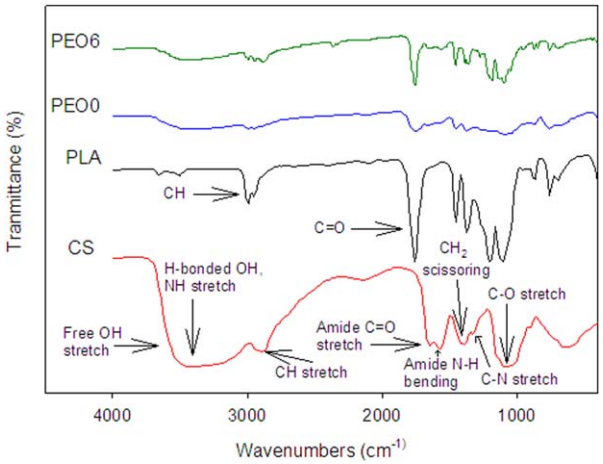

Figure 1. FTIR spectra of PLA, CS, PEO0, and PEO6. [Color figure can be viewed in the online issue, which is available at wileyonlinelibrary.com.]

C═O, C—O—C, OH groups in the PLA and the NH_2, C—O—C, OH groups in CS (mainly dipole interaction, hydrogen bonding, coordination linkage). Up to now, the works using of PEO as a compatibilizer for PLA/CS nanocomposites have not limited. Thus, in this study, the characteristics of PLA/CS/PEO nanocomposites including structure, morphology, thermal properties, and hydrolysis in acid and phosphate buffer solutions were reported and discussed. In addition, the regression equation for hydrolysis of PLA/CS/PEO nanocomposites tested in the solutions has been found.

EXPERIMENTAL

Materials

Poly (lactic acid) (PLA) (in pellets, degree of hydrolyzing > 99%, density of 1.25 g/cm^3, molecular weight of 1.42×10^4 Da, melt flow index of 7.75 g/10 min at 210°C, 2.16 kg) was purchased from NatureWorks LLC, USA. Chitosan (CS) (degree of deacetylation >77%, viscosity 1220 cPs, 1.61×10^5 Da) and PEO ($Mv = 100{,}000$, $T_g = 67.0$°C; polydispersity index PDI = $M_w/M_n = 1.02$–1.12, where M_w is the weight-averaged molecular weight) were obtained from Sigma-Aldrich, USA. Chloroform, hydrochloric acid (HCl), phosphate buffer solution are analytical reagents, which were used without further purification.

Preparation of PLA/CS/PEO Nanocomposites

PLA/CS and PLA/CS/PEO nanocomposites were prepared by solution method. Four hundred microgram PLA was dissolved in 25 mL chloroform to form a fine solution (solution A). CS at a concentration of 20 wt % in comparison with PLA [the suitable proportion of PLA and CS determined based on SEM images and DSC analysis is 80/20 (wt %/wt %)] was produced by dissolving the required amount of CS in solution of acetic acid 1% (v/v) at room temperature under magnetic stirring (solution B). PEO as compatibilizer was added to solution B at different ratio of 0, 2, 4, 6, 8, 10 wt % in comparison with PLA (solution C). Then, solution A and solution C were mixed by ultrasonic stirring for three times and 5 min/one time. The PLA/CS/PEO nanocomposites were obtained by solvent casting on a petri dish, followed by natural evaporation of the solvent at room temperature for 48 h and dried in avacuum oven at 40°C for 8 h. The prepared samples were abbreviated as PEO0; PEO2, PEO4, PEO6, PEO8, and PEO10 corresponding to 0–10 wt % of added PEO content, respectively.

Characterization

Fourier transform infrared (FTIR) spectra of PLA/CS and PLA/CS/PEO nanocomposites were recorded on a Nicolet/Nexus 670 spectrometer (USA) at room temperature by averaging 16 scans with a resolution of 4 cm^{-1} in transmission mode. The FTIR spectra were recorded in the wavenumbers range from 400 to 4000 cm^{-1}.

Field emission scanning electron microscopy (FE–SEM) of PLA/CS and PLA/CS/PEO nanocomposites coated by platinium was conducted using a S-4800 FE-SEM instrument (Hitachi, Japan).

Thermal property of PLA/CS and PLA/CS/PEO nanocomposites was performed on a DTG-60H and DSC-60 thermogravimetric analyzer (Shimadzu) under argon atmosphere from room temperature to 600°C at a heating rate of 10°C/min.

Determination of weight loss of the samples in phosphate buffer (pH = 7.4) and chloro hidric solutions (pH = 1) is based on the weight change after hydrolysis by the formular: $m = [(m_i - m_r)/m_i] \times 100\%$, in which m is loss weight of samples (%), m_i is the initial sample weight (g), and m_r is the retention weight of samples after hydrolysis (g).

RESULTS AND DISCUSSION

FTIR Spectra of PLA/CS/PEO Nanocomposites

Figure 1 presents FTIR spectra of chitosan (CS), PLA and PLA/CS (PEO0), PLA/CS/6 wt % PEO (PEO6) nanocomposites. The FTIR spectra of PEO2, PEO4, PEO8, PEO10 nanocomposites are similar to FTIR spectrum of PEO6 nanocomposite, therefore, they have not been showed here. CS is an amino glucose characterized by a small proportion of amide groups via an amide linkage with acetic acid. The IR spectrum of CS have a broad peak at 3426 cm^{-1}, which is assigned to the N—H and a peak at 3610 cm^{-1} corresponding to hydrogen bonded O—H

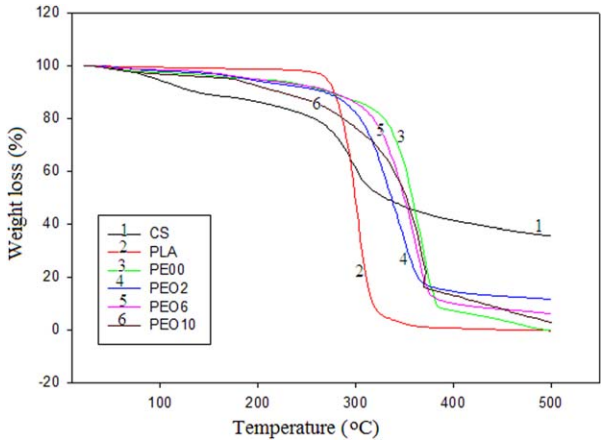

Figure 2. TG curvers of PLA, CS, and PLA/CS/PEO nanocomposites. [Color figure can be viewed in the online issue, which is available at wileyonlinelibrary.com.]

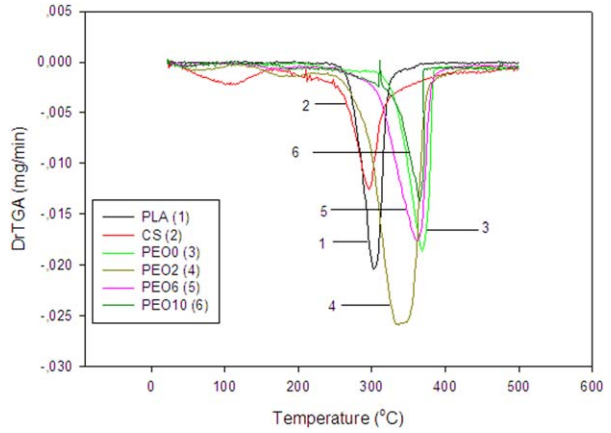

Figure 3. DTG thermograms of PLA, CS, and PLA/CS/PEO nanocomposites. [Color figure can be viewed in the online issue, which is available at wileyonlinelibrary.com.]

Table II. DSC Data of PLA, CS, PLA/CS, and PLA/CS/PEO Nanocomposites

Samples	T_g (°C)	T_m (°C)	ΔH_m (J/g)	χ_c[a] (%)
PLA	54.7	150.5	8.5	9.1
CS	-	-	-	-
PEO0	64.3	157.3	10.8	11.6
PEO2	68.6	150.6	11.5	12.4
PEO4	62.9	150.3	12.8	13.7
PEO6	69.0	150.6	16.5	17.7
PEO8	68.5	150.5	16.0	17.2
PEO10	68.2	150.1	15.4	16.5

T_g: glass transition temperature; T_m: melting temperature; ΔH_m: enthalpy of melting.
[a] χ_c (%) = $\Delta H_m \times 100/\Delta H_m$ where ΔH_m is the heat of fusion for completely crystallized PLA (93.1 J/g).[2]

stretch vibrational frequencies with a sharp (shoulder). This indicates the free O—H bond stretch of glucopyranose units.[3] In the C—H stretch region of CS in FTIR spectrum, a peak at 2888 cm^{-1} is assigned to the vibration of CH_2. In addition, the characteristic band due to CH_2 scissoring, which usually occurs at 1465 cm^{-1} is also present in this spectrum. Moreover, the C═O stretch of amide bond is observed at 1670 cm^{-1}, and a peak at 1581 cm^{-1} is assigned to strong N—H bending vibration of secondary amide, which usually occurs in the range of 1640–1550 cm^{-1} as strong band. Besides, the C—O asymmetric and symmetric stretchs are found at 1153 and 1091 cm^{-1}.[3,9] Several characteristic bands of PLA (Figure 1) are located at 677 cm^{-1} (753 and 866 cm^{-1}) (aldehydic CH stretching); 1101 and 1199 cm^{-1} (C—O stretch); 1368 and 1452 cm^{-1} (CH_2, CH_3 bending); 1759 cm^{-1} (C—O stretch, ester group); 2991 and 2945 cm^{-1} (CH_3, CH stretch); and 3680 cm^{-1} (free —OH stretch, end group).[2,9] It is clear that two noticeable changes occur in the spectrum of PLA/CS nanocomposite (PEO0). An original strong band of the PLA component at 1759 cm^{-1} for the ester group becomes significantly weaker and markedly wider. The intensity of stretching bands overlapped and centered near 3426 cm^{-1} for the hydroxyl and amino groups pronouncedly decreases to 3366 cm^{-1}. The above data of FTIR spectra indicate that there are obvious weak interactions among amino, carboxyl, and hydroxyl groups of PLA and CS. Similar results were also reported in the study of PLA/CS nanoparticles of D. Jeevitha *et al.*[9] in which the hydrogen bonds were formed between amino and hydroxyl groups (in CS) and carboxyl groups (in PLA) and there is no covalent interaction between PLA and CS chains. Interestingly, in the FTIR spectra of PLA/CS/PEO nanocomposites, all peaks in the FTIR of PEO6 exhibit clearer with a stronger intensity and slight shift than those of PEO0. This proves that PLA interacted with CS better in the presence of PEO as a compatibilizer which is metioned by Rajan *et al.*[11]

Thermal Property of PLA/CS/PEO Nanocomposites

TGA. Thermal properties of PLA, CS, PLA/CS, and PLA/CS/PEO nanocomposites were studied by TGA/DTG and DSC analysis. It can be seen that CS has a two-stage degradation pattern in TG curvers (Figure 2). It may be attributed to the thermal evaporation of bound water (which could not be removed completely on drying) and thermo-degradation of the CS chains.[14–16] The TG curvers of PLA/CS/PEO nanocomposites are similar to those of PLA with a one-stage of thermo-degradation. Their DTG thermograms display only one value of maximal temprerature of thermo-degradation (T_{max}) coressponding to the thermo-degradation of hidrocarbon chain of PLA (Figure 3). Interestingly, the T_{onset} value of PLA/CS/PEO

Table I. T_{onset}, T_{max}, and Weight Loss of PLA, CS, PLA/CS/PEO Nanocomposites versus Heating Temperature

	Weight loss (%)							
Temperature (°C)	PLA	CS	PEO0	PEO2	PEO4	PEO6	PEO8	PEO10
250	2.13	21.50	9.92	13.52	12.60	11.62	12.93	15.10
300	48.77	41.39	15.62	22.30	21.20	17.83	23.06	25.45
350	97.82	55.00	39.62	67.59	71.71	53.40	55.70	50.69
400	99.45	60.07	93.09	86.27	88.82	90.88	85.71	81.36
450	100.00	63.20	96.58	88.01	90.51	92.59	89.53	92.38
T_{onset}	300.06	198.95	269.52	272.77	273.25	270.36	275.08	276.12
T_{max}	303.87	109.40, 296.90	369.01	337.06	349.38	361.72	360.71	365.08

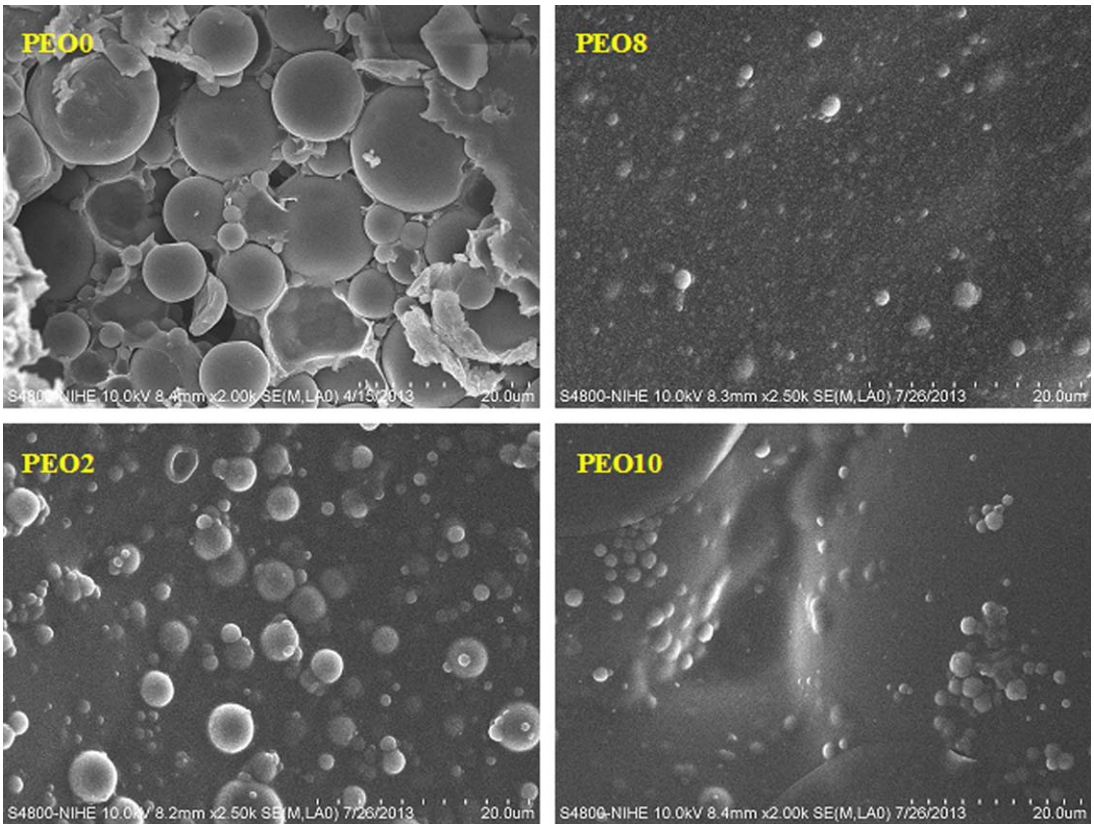

Figure 4. FESEM images of PLA/CS/PEO nanocomposites (PEO0, PEO2, PEO8, PEO10 correspond the samples using 0, 2, 8, and 10 wt % PEO). [Color figure can be viewed in the online issue, which is available at wileyonlinelibrary.com.]

nanocomposites is shifted to higher temperature in comparison with that of PLA/CS sample (Table I). This proves that PEO play an important role in improving thermal stability of the PLA/CS sample due to improve disperibility and compatibility between PLA and CS.[11,14,15] The increase in thermal stability clearly observed for the PLA/CS/PEO nanocomposites at the temperature higher than 380°C. This can be proved by lower weight loss of PLA/CS/PEO nanocomposites at different heating temperatures (Table I). The TG curvers and DTG thermograms of PEO4 and PEO8 samples are similar to PEO2, PEO6, PEO10 samples and they are not presented here.

DSC. The DSC data display two endothermic peaks are attributed to the glass transition (T_g) and melting process of PLA, PLA/CS, and PLA/CS/PEO nanocomposites with different content of PEO. Pure chitosan does not have melting properties and hence no endothermic peaks associated to melting process were detected.[17] This obtained result is similar to the reports of

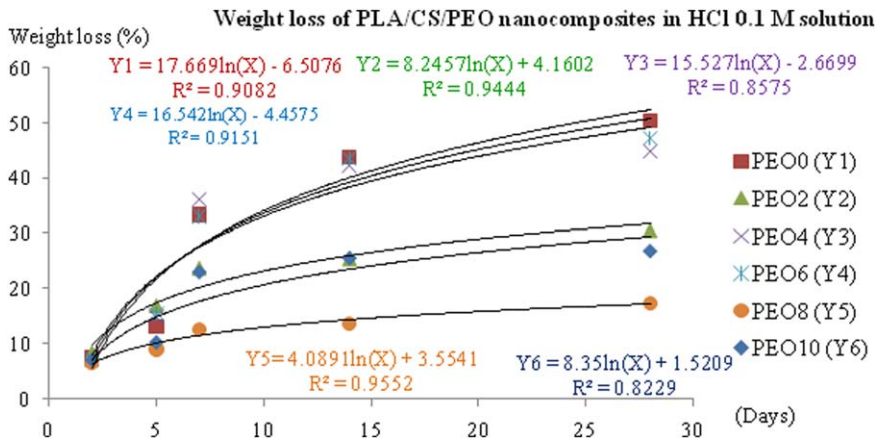

Figure 5. Weight loss of PLA/CS/PEO nanocomposites versus immersion time and regression equation reflecting the weight loss (Y %) of the samples versus immersion time (X-days) in HCl 0.1*M* solution. [Color figure can be viewed in the online issue, which is available at wileyonlinelibrary.com.]

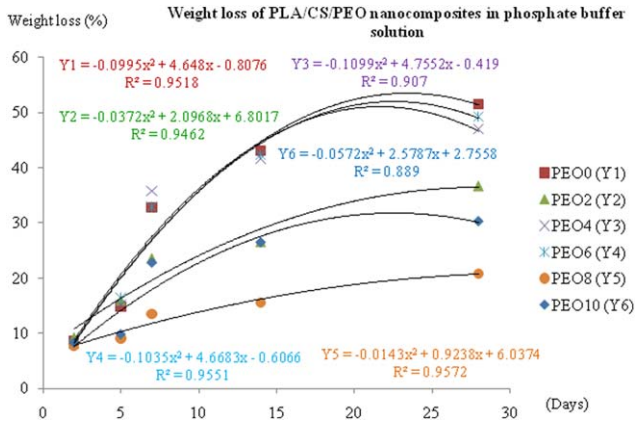

Figure 6. Weight loss of PLA/CS/PEO nanocomposites versus immersion time and regression equation reflecting the weight loss (Y %) of the samples versus immersion time (X-days) in phosphate buffer (pH = 7.4) solution. [Color figure can be viewed in the online issue, which is available at wileyonlinelibrary.com.]

Constantin Edi Tanase *et al.*,[17] Manisara Peesan *et al.*,[18] and Bonilla *et al.*[19] It is known that the T_g is a complex phenomenon, which depends on several factors including intermolecular interactions, steric effects, the chain flexibility, the molecular weight, the branching, and the crosslinking density.[20] Here, by the addition of CS and PEO into PLA, the T_g is shifted to higher temperatures and the relative crystallinity (χ_c) increase in comparison with the T_g of neat PLA (Table II). It means the presence of CS and PEO can lead to the rearrangement of crystal structure of PLA, the polymer phase compatibility took place between the two polymers when using PEO as a compatibilizer.[21,22]

Morphology of PLA/CS/PEO Nanocomposites

Figure 4 demonstrates FESEM images of PLA/CS and PLA/CS/PEO nanocomposites using different PEO content. It can be seen that these nanocomposites exhibit two phases including a matrix phase and a spherical dispersion phase. Clearly, PLA is poor compatible with CS in PEO/CS sample without PEO (PEO0). The dispersion CS phase appears with irregular size in a range of 1–14 μm in PLA matrix. The morphology of PLA/CS/PEO nanocomposites using different PEO content (PEO2, PEO8, and PEO10) seems more regular and the dispersion phase has smaller size, maintly, from 100 nm to 2 μm. This can be explained by the presence PEO, which plays an important role in improvement the dispersibility and compatibility between PLA and CS thought the mentioned physical interactions in sections "FTIR Spectra of PLA/CS/PEO Nanocomposites" and "Thermal Property of PLA/CS/PEO Nanocomposites."

Hydrolysis of PLA/CS/PEO Nanocomposites in Some Different Solutions

Two main factors affected the hydrolysis of PLA and PLA/CS/PEO nanocomposites in HCl and phosphate buffer solutions

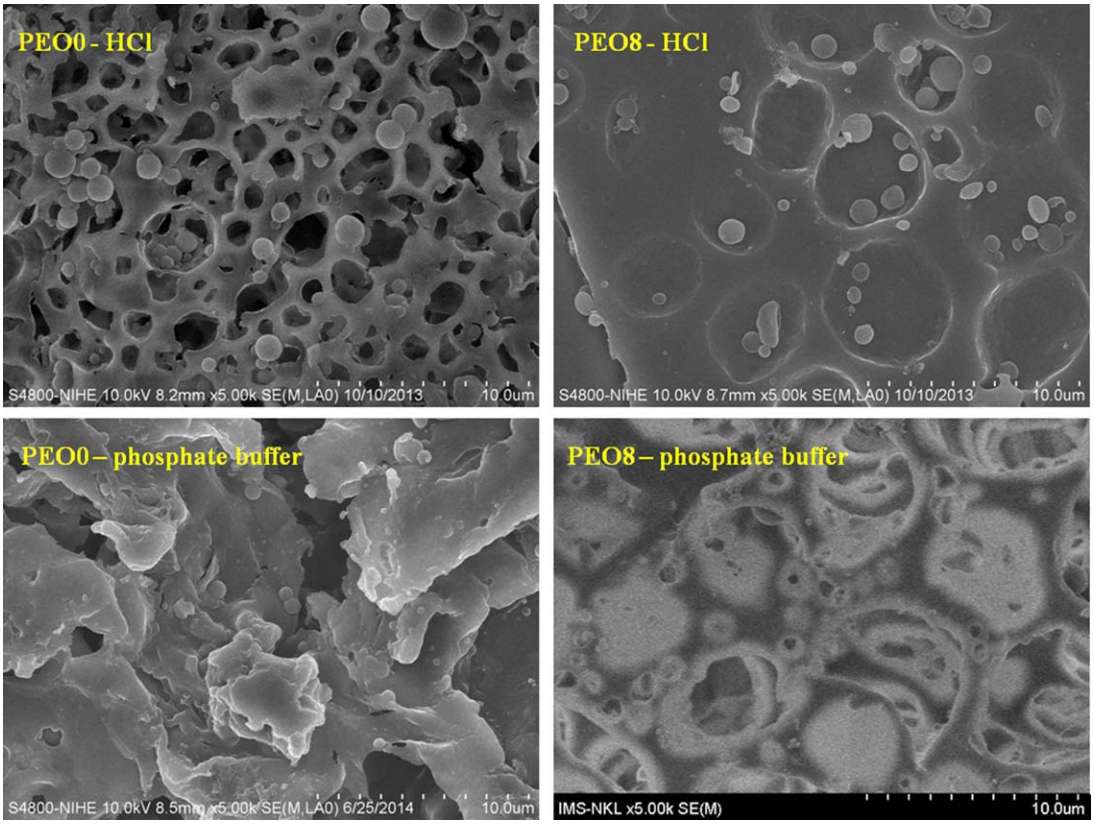

Figure 7. FESEM images of PEO0 and PEO8 nanocomposites after 28 days of immersion in HCl 0.1*M* and phosphate buffer (pH = 7.4) solution. [Color figure can be viewed in the online issue, which is available at wileyonlinelibrary.com.]

are water and self-catalytic mechanism.[23,24] Figures 5 and 6 present results of weight loss of PLA/CS and PLA/CS/PEO nanocomposites versus immersion time and regression equation reflecting the weight loss (Y %) of the samples versus immersion time (X-days) in HCl 0.1*M* and phosphate buffer (pH = 7.4) solutions. The weight loss of the both PLA/CS and PLA/CS/PEO nanocomposites in phosphate buffer solution is higher than that in HCl solution. It could be caused by OH^- agent in the phosphate buffer solution is very strong nucleofin agent, it can lead to rapid hydrolysis of PLA. The PLA component in PLA/CS and PLA/CS/PEO nanocomposites was hydrolyzed to form holes in the materials (seen in Figure 7). It is exhibited clearly through the change in structure and morphology of the samples after 28 immersion days. The structure of PLA/CS and PLA/CS/PEO6 nanocomposite after 28 immersion days in phosphate buffer solution was destroyed stronger than in HCl 0.1*M* solution. The PLA/CS/PEO nanocomposites were hydrolyzed slower than PLA/CS composite in both solutions. Once again, this result affirms the role of PEO in improvement the compatibility between PLA and CS and the closer structure of PLA/CS/PEO nanocomposites in comparision with PLA/CS composite. As a result, the PLA/CS composite was destroyed stronger than the PLA/CS/PEO nanocomposites with more holes in its structure. The weight loss of the nanocomposites is different and irregular due to the improvement of compatibility between PLA and CS at some PEO contents.

The regression equations reflecting the weight loss of the samples versus hydrolysis time in HCl 0.1*M* and phosphate buffer (pH = 7.4) solutions are also presented in Figures 5 and 6. Among of the investigated samples in HCl 0.1*M* solution, the regression equation $Y5 = 4.0891\ln(X) + 3.5541$ (for PEO8 sample) has the largest regression coefficient ($R^2 = 0.9552$). For the case in phosphate buffer (pH = 7.4) solution, the regression equation $Y5 = -0.0143x^2 + 0.9238x + 6.0374$ (for PEO8 sample) has largest regression coefficient ($R^2 = 0.9572$).

CONCLUSION REMARKS

In conclusion, the FTIR spectra of PLA, CS, PLA/CS composite, and PLA/CS/PEO nanocomposites show the existence of interactions between characterized functional groups in PLA, CS, and PEO. TG/DTG and DSC analysis results proved the compatibility between the PLA and CS in the presence of PEO as a compatibilizer, leading to the increase of degree of crystallinity for all PLA/CS/PEO nanocomposites. At high temperature, PEO and CS improved the thermal stability of PLA. FESEM images of the nanocomposite indicate also that PEO enhances the compatibility between PLA and CS and more regular dispersion of CS in PLA. The weight loss of PLA/CS composite and PLA/CS/PEO nanocomposites in the phosphate buffer (pH = 7.4) solution is higher than in the HCl 0.1*M* solution. The regression equation for hydrolysis process of the PEO8 nanocomposites in phosphate buffer (pH = 7.4) solution is $Y5 = -0.0143x^2 + 0.9238x + 6.0374$ with the largest regression coefficient of 0.9572 and in HCl 0.1*M* solution is $Y5 = 4.0891\ln(X) + 3.5541$ with the largest regression coefficient of 0.9552.

ACKNOWLEDGMENTS

The authors would like to thank the National Foundation for Science and Technology Development of Vietnam (Subject of fumdamental research and applied orientation, the period of 2013–2016, code DT.NCCB-DHUD.2012-G/09) for the financial support.

REFERENCES

1. Henton, D. E.; Gruber, P.; Lunt, J.; Randall, J. In: Natural fibers, biopolymers and biocomposites; Moharty, A. K., Mishra, M., Drzal, L. T., Eds.; Taylor & Francis: Boca Raton, FL, **2005**, 527–577.
2. Kumar, R.; Muzzarelli, R. A. A.; Muzzarelli, C.; Sashiwa, H. *Chem. Rev.* **2004**, *104*, 6017.
3. Kurita, K. *Prog. Polym. Sci.* **2001**, *26*, 1921.
4. Liao, Y. Z.; Xin, M. H.; Li, M. C.; Su, S. *Chin. Chem. Lett.* **2007**, *18*, 213.
5. Prabaharan, M.; Rodriguez-Perez, M. A.; De Saja, J. A.; Mano, J. F. *J. Biomed. Mater. Res. B: Appl. Biomater.* **2007**, *81*, 427.
6. Zhang, X.; Hua, H.; Shen, X.; Yang, Q. *Polymer* **2007**, *48*, 1005.
7. Dev, A.; Binulal, N. S.; Anitha, A.; Nair, S. V.; Fruike, T.; Tamura, H.; Jayakumar, R. *Carbohydr. Polym.* **2010**, *80*, 833.
8. Nanda, R.; Sasmal, A.; Nayak, P. L. *Carbohydr. Polym.* **2011**, *83*, 988.
9. Jeevitha, D.; Kanchana, A. *Colloids Surf. B* **2013**, *101*, 126.
10. Lee, J. W.; Jeong, E. D. *Appl. Surf. Sci.* **2008**, *255*, 2360.
11. Rajan, M.; Raj, V. *Carbohydr. Polym.* **2013**, *98*, 951.
12. Cohn, D.; Hotovely Salomon, A. *Biomaterials* **2005**, *26*, 2297.
13. Hoang, T.; Trang, N. T. T.; Chinh, N. T. *Vietnam J Chem* **2012**, *50*, 570.
14. Bonilla, J.; Fortunati, E.; Vargas, M.; Chiralt, A.; Kenny, J. M. *J. Food Eng.* **2013**, *119*, 236.
15. Tripathi, S.; Mehrotra, G. K.; Dutta, P. K. *Int. J. Biol. Macromol.* **2009**, *45*, 372.
16. Paulino, A. T.; Simionato, J. I.; Garcia, J. C.; Nozaki, J. *Carbohydr. Polym.* **2006**, *64*, 98.
17. Constantin Edi, T.; Iuliana, S. *Mater. Sci. Eng. C* **2014**, *40*, 242.
18. Manisara, P.; Pitt, S.; Ratana, R. *Carbohydr. Polym.* **2005**, *60*, 343.
19. Bonilla, J.; Fortunati, E.; Vargas, M.; Chiralt, A.; Kenny, J. M. *J. Food Eng.* **2013**, *119*, 236.
20. Fronea, A. N.; Berliozb, S.; Chailanb, J. F.; Panaitescu, D. M. *Carbohydr. Polym.* **2013**, *91*, 377.
21. Naveen Kumara, H. M. P.; Prabhakar, M. N.; Venkata Prasad, C.; Madhusudhan Rao, K.; Ashok Kumar Reddy, T. V.; Chowdoji Rao, K.; Subha, M. C. S. *Carbohydr. Polym.* **2010**, *82*, 251.
22. Chouzouri, G.; Xanthos, M. *J. Plast. Film Sheet.* **2007**, *23*, 19.
23. Tsuji, H.; Nakahara, K. *J. Appl. Polym. Sci.* **2002**, *86*, 186.
24. Yuan, X. Y.; Mark, A. F. T.; Yao, K. *Polym. Degrad. Stab.* **2002**, *75*, 45.